SEDIMENTOLOGY the journal of the International Association of Sedimentologists IAS

Sedimentology (2024) doi: 10.1111/sed.13179

Organic matter influence on ooid formation: New insights into classic examples (Great Salt Lake, USA; Triassic Germanic Basin, Germany)

YU PEI*,†,‡, PABLO SUAREZ-GONZALEZ§, JAN-PETER DUDA‡,¶ and JOACHIM REITNER‡,¶

**State Key Laboratory of Biogeology and Environmental Geology, China University of Geosciences (Wuhan), Lumo Road 388, Wuhan 430074, China (E-mail: peiyu@cug.edu.cn)*

†Department of Geosciences, Eberhard Karls Universität Tübingen, Schnarrenbergstrasse 94-96, Tübingen 72076, Germany

‡'Origin of Life' Group, Göttingen Academy of Sciences and Humanities, Theater Strasse 7, Göttingen 37073, Germany (E-mail: jreitne@gwdg.de)

§Departamento de Geodinámica, Estratigrafía y Paleontología, Complutense University of Madrid, José Antonio Nováis 12, Madrid 28040, Spain

¶Department of Geobiology, Geoscience Center, Georg-August-Universität Göttingen, Goldschmidtstrasse 3, Göttingen 37077, Germany

Associate Editor – Stephen Lokier

ABSTRACT

Ooids are coated grains composed of a tangential or radial cortex growing around a nucleus. They are common in carbonate deposits of almost any geological age and provide insights into environmental conditions. However, abiotic or biotic factors influencing their formation remain unclear. This study aims to advance current understanding of ooid formation with a multi-analytical approach (for example, field emission scanning electron microscopy, Raman spectroscopy and micro X-ray fluorescence) to classic examples from Great Salt Lake, USA, and the Lower Triassic Germanic Buntsandstein Basin, Germany. Both of these deposits represent hypersaline shallow-water environments where ooids are closely associated with microbial mats. Great Salt Lake ooids are dominantly 0.2 to 1.0 mm in size, ellipsoidal to subspherical in shape, composed of aragonite and contain organic matter. Germanic Buntsandstein Basin ooids are mainly ≤4 mm in size, spherical to subspherical in shape, composed of calcite and currently contain little organic matter. Despite the differences, both ooids have the same cortex structures, likely reflecting similar formation processes. Some Great Salt Lake ooids formed around detrital grains while others exhibit micritic particles in their nuclei. In Germanic Basin ooids, detrital nuclei are rare, despite the abundance of siliciclastic particles of various sizes in the host rocks. Germanic Basin deposits also include 'compound ooids', i.e. adjacent ooids that coalesced with one another during growth, suggesting static *in situ* development, which is supported by the lack of detrital grains as nuclei. Germanic Basin ooids also grew into laminated microbial crusts with identical microstructures, further indicating a static formation. Such microbial crusts typically form through mineral precipitation associated with organic matter (for example, extracellular polymeric substances), suggesting a similar formation pathway for ooids. The inferred key-role of organic matter is further supported by features in radial ooids from the Great Salt Lake, which commonly exhibit, from their nuclei towards their surface, increasing organic matter contents and decreasing calcification.

Keywords Cortex, extracellular polymeric substances, laminae, mineralization, organic matter, organomineralization.

INTRODUCTION

Ooids are significant particles of carbonate deposits from many different sedimentary environments since the Archaean (e.g. Kalkowsky, 1908; Davies *et al.*, 1978; Simone, 1981; Krumbein, 1983; Summons *et al.*, 2013; O'Reilly *et al.*, 2017; Siahi *et al.*, 2017; Mariotti *et al.*, 2018; Diaz & Eberli, 2019; Flannery *et al.*, 2019). They are typically characterized by tangential and/or radial cortices and have sizes of <2 mm (Richter, 1983; Flügel, 2010). In addition to the Precambrian, ooids are relatively common in critical junctures in the Phanerozoic, for example, after the Permian–Triassic catastrophe. Ooids, especially giant ooids (>2 mm), are relatively common during these periods (e.g. Sumner & Grotzinger, 1993; Li *et al.*, 2015, 2021). Ooids have caught the attention of humans since prehistoric times (Binsteiner *et al.*, 2008; Weber *et al.*, 2022) and were already mentioned by Roman naturalists (Burne *et al.*, 2012). However, their first scientific description was provided in a treatise devoted entirely to the ooids of the Lower Buntsandstein (Lower Triassic) from northern and central Germany by Brückmann (1721), who followed Volkmann (1720) in using the Greek word 'oolithos' (literally 'egg-rock', due to their similarity to fish roe), a translation of the German 'Rogenstein' or 'Eierstein' (Burne *et al.*, 2012). In the landmark book on the microfacies of carbonate rocks, Flügel (2010) defined ooids as: "spherical and egg-shaped carbonate or non-carbonate coated grains exhibiting a nucleus surrounded by an external cortex, the outer part of which is concentrically smoothly laminated".

Despite this long history of research, the formation process of ooids still remains disputed and unresolved, and both inorganic and organic hypotheses have been proposed. The inorganic hypothesis involves a direct precipitation of aragonite or calcite from fluids supersaturated with respect to $CaCO_3$ (e.g. Illing, 1954; Sumner & Grotzinger, 1993; Duguid *et al.*, 2010; Paul *et al.*, 2011; Trower *et al.*, 2017, 2018). In this model, larger ooids are predicted to result from faster precipitation rates promoted by a higher calcium carbonate saturation state, combined with increased agitation to allow larger grains to be transported for active growth (Trower *et al.*, 2017; Li *et al.*, 2021). In the organic hypothesis, aragonite or calcite precipitation is closely associated with microbial extracellular polymeric substances (EPS), which consist of complex mixtures of various organic compounds such as polysaccharides, proteins, nucleic acids and lipids (Flemming & Wingender, 2010; Flemming, 2016; Decho & Gutierrez, 2017). EPS are widespread in biofilms (Wingender *et al.*, 1999; Flemming *et al.*, 2007; Neu & Lawrence, 2010), implying the presence of a rich and diverse community of microorganisms during ooid formation (Friedmann *et al.*, 1973; Gerdes *et al.*, 1994; Brehm *et al.*, 2006; Plée *et al.*, 2008; Summons *et al.*, 2013; Woods, 2013; Diaz *et al.*, 2015, 2017; O'Reilly *et al.*, 2017; Hubert *et al.*, 2018). Microorganisms are put forward to induce carbonate precipitation by their metabolic activity. However, living microorganisms must not necessarily be directly involved, because carbonate precipitation can also be linked to degraded organic matter (OM) ('Organomineralization': Mitterer, 1968; Suess & Fütterer, 1972; Ferguson *et al.*, 1978; Trichet & Défarge, 1995; Reitner *et al.*, 1995a,b, 1997; Reitner, 2004).

Herein, Lower Triassic ooids from the Germanic Basin, Germany, and modern counterparts from the Great Salt Lake, USA, were studied and compared. Ooids from both localities have been continuously studied since the XIX century until now (e.g. Rothpletz, 1892; Kalkowsky, 1908; Käsbohrer & Kuss, 2019, 2021; Ingalls *et al.*, 2020, Trower *et al.*, 2020) and have been central for the development of early hypotheses about the organic influence on ooid formation (e.g. Kalkowsky, 1908, for Germanic Buntsandstein Basin ooids; Rothpletz, 1892, for Great Salt Lake ooids). Although more than a century has passed since those early hypotheses, much remains unknown about the exact role of OM in forming ooids. This work aims at advancing that direction by analysing the similarities and differences between ooids from the very same classic localities that originated the idea of organic influence on ooids, and by discussing their possible formation processes.

MATERIALS AND METHODS

Geological setting and sample material

The Early Triassic Buntsandstein Group was deposited in the Germanic Buntsandstein Basin, which extended from England to Belarus and from Denmark to Germany (Fig. 1A and B). It was mainly a continental basin but occasionally connected to the western Tethys Ocean (Meliata Ocean), and characterized by subtropical to arid climates (Ziegler, 1990; Stampfli, 2000; Weidlich, 2007; Scholze *et al.*, 2017; Scotese, 2021). This study focuses on the Lower Buntsandstein Subgroup in Germany (Fig. 1B). The subgroup can be up to *ca* 450 m thick, consisting of siliciclastic rocks intercalated with carbonates (Ziegler, 1990). It is further subdivided into the Calvörde and Bernburg formations. The studied ooids and stromatolites occur in the Bernburg Formation. They may have formed in a lacustrine environment characterized by elevated salinities (Paul & Peryt, 2000; Käsbohrer & Kuss, 2019), although some studies favour a marine environment due to a transgression (Weidlich, 2007). In addition to materials sampled during various field campaigns

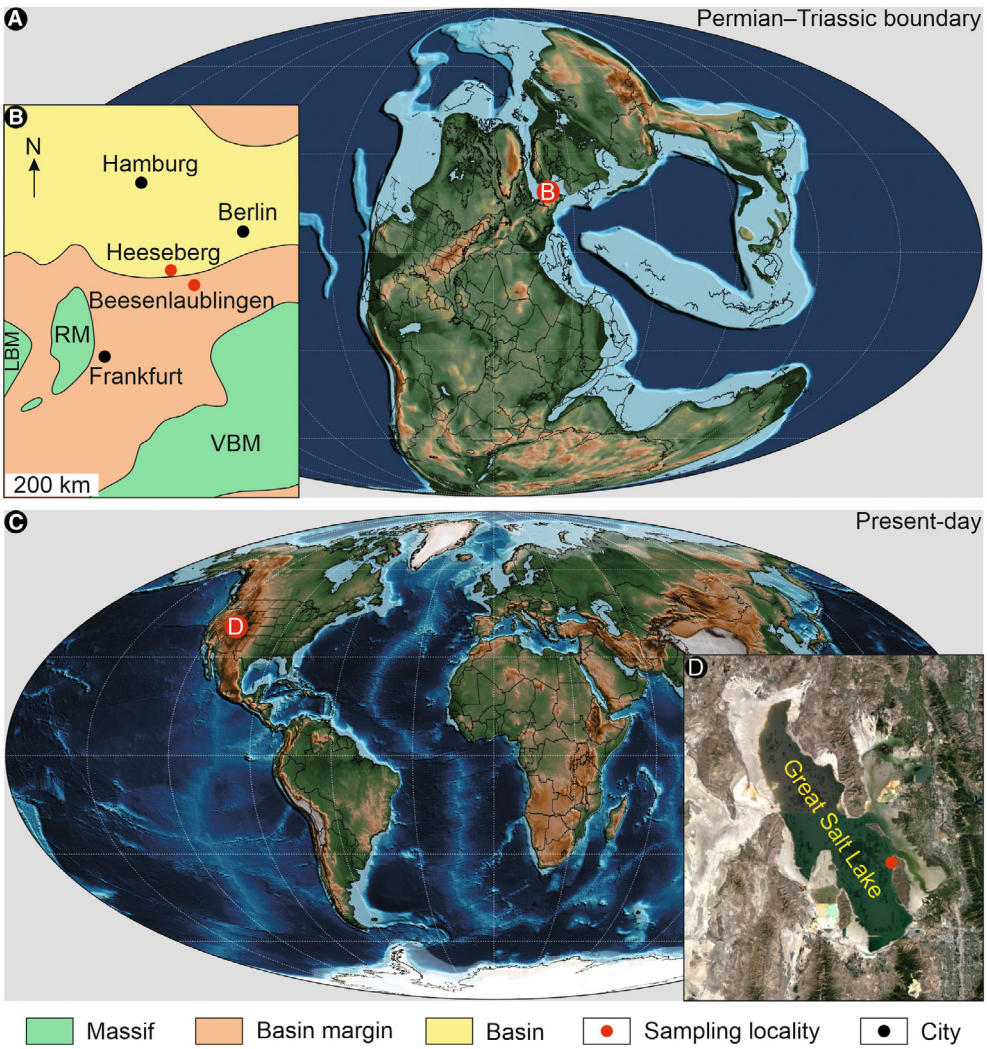

Fig. 1. (A) Palaeogeographical map of Permian–Triassic boundary (*ca* 250 Ma ago, Scotese, 2021). (B) Palaeogeography of the Lower Buntsandstein Subgroup (Early Triassic) in Germany (modified from Scholze *et al.*, 2017) with main modern cities marked in black and the two sampling localities in red. LBM, London – Brabant – Massif; RM, Rhenish Massif; VBM, Vindelician – Bohemian – Massif. (C) Geographic map of Present-day (Scotese, 2021). (D) Geographic position of the sampling locality in red at the north-western coast of Antelope Island in the Great Salt Lake (Google Earth Pro image).

between 2018 and 2020 at the Heeseberg and surroundings, and in Beesenlaubingen (Fig. 1B), existing samples that are archived in the Göttingen Geoscience Collections at the University of Göttingen were studied.

The Great Salt Lake, USA, is an endorheic lake (Fig. 1C) and a remnant of the Pleistocene Lake Bonneville (Oviatt *et al.*, 1999; Shroder *et al.*, 2016). Its salinity varies from approximately 12 to 26%, with Na^+ and Cl^- being the major ions. The studied modern ooids were sampled at the north-western coast of Antelope Island in 1994 and 1996 (Fig. 1D), where the salinity is 12 to 14% (Chidsey *et al.*, 2015). The samples are now stored in the Göttingen Geoscience Collections at the University of Göttingen.

Sample preparation

Petrographic thin sections were prepared from the Triassic samples of the Germanic Basin. Modern ooid samples from Great Salt Lake were processed directly after sampling in the field. Some samples were fixed in buffered formalin, dehydrated and stored in 70% ethanol, while others were fixed in buffered glutardialdehyde (cooled on ice for 24 h) and postfixed with 2% osmium tetroxide (for details see Reitner, 1993). All Great Salt Lake samples were then stained with Ca^{2+}-chelating fluorescent dye (for example, calcein) and non-fluorescent dye (for example, alcian blue). Subsequently, thin sections were prepared from LR White-embedded specimens with a Leica SP 1600 saw microtome (Leica Microsystems, Wetzlar, Germany).

Petrography and analytical imaging

Thin sections were analysed using a Zeiss SteREO Discovery.V12 stereomicroscope and a Zeiss AXIO Imager.Z1 microscope (Carl Zeiss AG, Oberkochen, Germany). Photographs were taken with an AxioCamMRc 5 MB camera.

For epifluorescence microscopy, a Zeiss AXIO Imager.Z1 microscope was utilized. It is equipped with a high-pressure mercury arc lamp (HBO 50, Zeiss; controlled by an EBX 75 ISOLATED electronic transformer) and a 10 AF488 filter (excitation wavelength = BP 450–490 nm, emission wavelength = BP 515–565 nm). Thin sections with Ca^{2+}-chelating fluorescent dye were studied with a ZEISS Axioplan using a high performance wide-band pass filter (blue, BP 450–490, LP 520; no. 487709) (for details see Hicks & Matthaei, 1958; Reitner, 1993).

For field emission scanning electron microscopy (FE-SEM), a Carl Zeiss LEO 1530 Gemini system was used. Some thin sections of the modern samples were etched by submerging them in a 5% ethylenediaminetetraacetic acid (EDTA) solution for 10 to 30 s.

A Bruker M4 Tornado instrument (Bruker, Billerica, MA, USA) equipped with an XFlash 430 Silicon Drift Detector was used for micro X-ray fluorescence (μ-XRF) to obtain element distribution images of thin sections. Measurements (spatial resolution = 25 μm, pixel time = 8 ms) were conducted at 50 kV and 400 μA with a chamber pressure of 20 mbar.

A WITec alpha300 R fibre-coupled ultra-high throughput spectrometer (Oxford Instruments, Abingdon, UK) was employed to collect Raman single spectra and spectral images to analyse mineral compositions of thin sections. Before analysis, the system was calibrated employing an integrated light source. For both single spectra and spectral images, the experimental setup includes a 532 nm excitation laser, an automatically controlled laser power of 20 mW, a 100 × long working distance objective with a numerical aperture of 0.75 and a 300 g mm^{-1} grating. The spectrometer was centred at 2220 cm^{-1}, covering a spectral range from 68 to 3914 cm^{-1}. This setup has a spectral resolution of 2.2 cm^{-1}. For single spectra, each was collected by two accumulations, with an acquisition time of 2 s. For spectral images, spectra were collected at a step size of 1 μm in horizontal and vertical directions by an acquisition time of 0.25 s for each spectrum. Automated cosmic ray correction, background subtraction and fitting using a Lorentz function were performed using the WITec Project software. Raman images were additionally processed with spectral averaging/smoothing and component analysis.

RESULTS

Lower Triassic ooids from the Germanic Basin

In the working area, the Bernburg Formation consists of siliciclastic and carbonate rocks (for example, floatstone after Lokier & Al Junaibi, 2016) which show abundant sedimentary structures (for example, cross-bedding, climbing ripples and wave ripples). A prominent feature of the formation are stromatolites with columnar growth forms and thicknesses of 10 to 50 cm

(rarely up to 1.2 m) (Fig. 2A and B). Ooids in the Bernburg Formation are typically large with diameters exceeding 2 mm (Fig. 2C and D; see below for details). In many oolitic beds, ooids are overgrown by thin, 5 to 50 cm wide microbial crusts. Notably, these crusts show a lamination equivalent to that of the ooids. They either develop into a thicker stromatolite bed or are overlaid by another oolitic bed (Fig. 2C and D).

Morphology and composition

The Germanic Buntsandstein Basin ooids are up to 4 mm in diameter and spherical to subspherical in shape. Their nuclei are most commonly dark micritic particles (for example, Fig. 3A) even though detrital (for example, quartz) grains of various sizes are abundant in the sediment (for example, Figs 4A, 5 and 6). Four types of ooids are distinguished, according to the structure of their cortices. Type A ooids show co-occurring radial and tangential structures across their cortices (Fig. 3A). Type B ooids exhibit alternating radial and tangential features (Fig. 3B). Type C ooids are radial showing indistinct laminae (Fig. 3C). Type D ooids are tangential exhibiting indistinct radial features (Fig. 3D). Among the four types, Type A ooids are the most prominent. Type C ooids are typically smaller in size (<0.5 mm) and can occur as the initial stage of other types of ooids. In some cases, adjacent ooids have coalesced during growth, forming 'compound ooids', which are very common in some samples (Fig. 3E and F).

Both radial and tangential cortices exhibit a relatively strong green fluorescence, which is typically brighter in the darker radial segments and darker laminae (Fig. 3G and H). Raman spectroscopy shows that the ooids are mainly

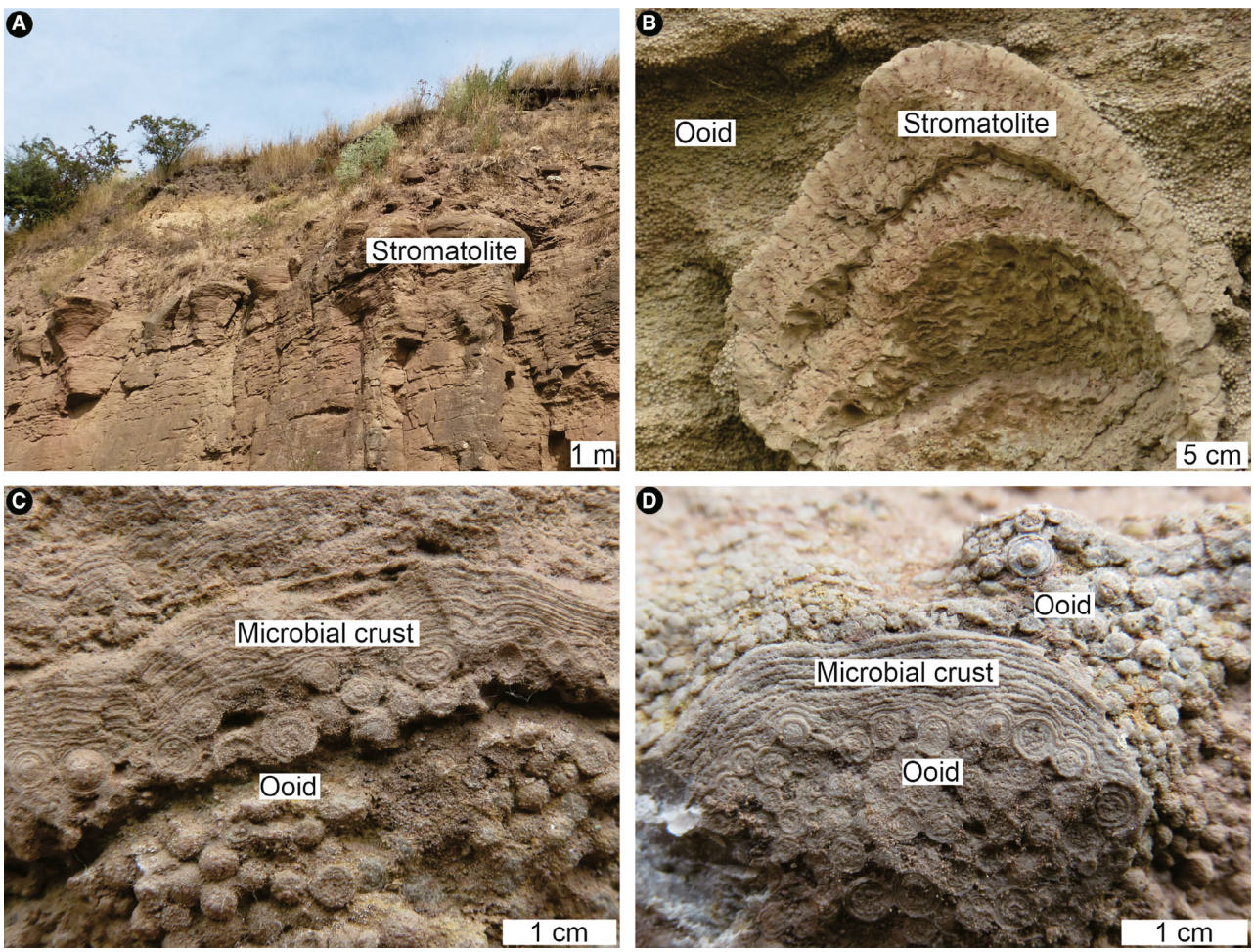

Fig. 2. Field pictures of the Early Triassic, the Germanic Basin. (A) and (B) Oolitic deposits alternate with columnar stromatolites. (C) and (D) The giant ooids, diameter >2 mm, are overlaid by microbial crusts.

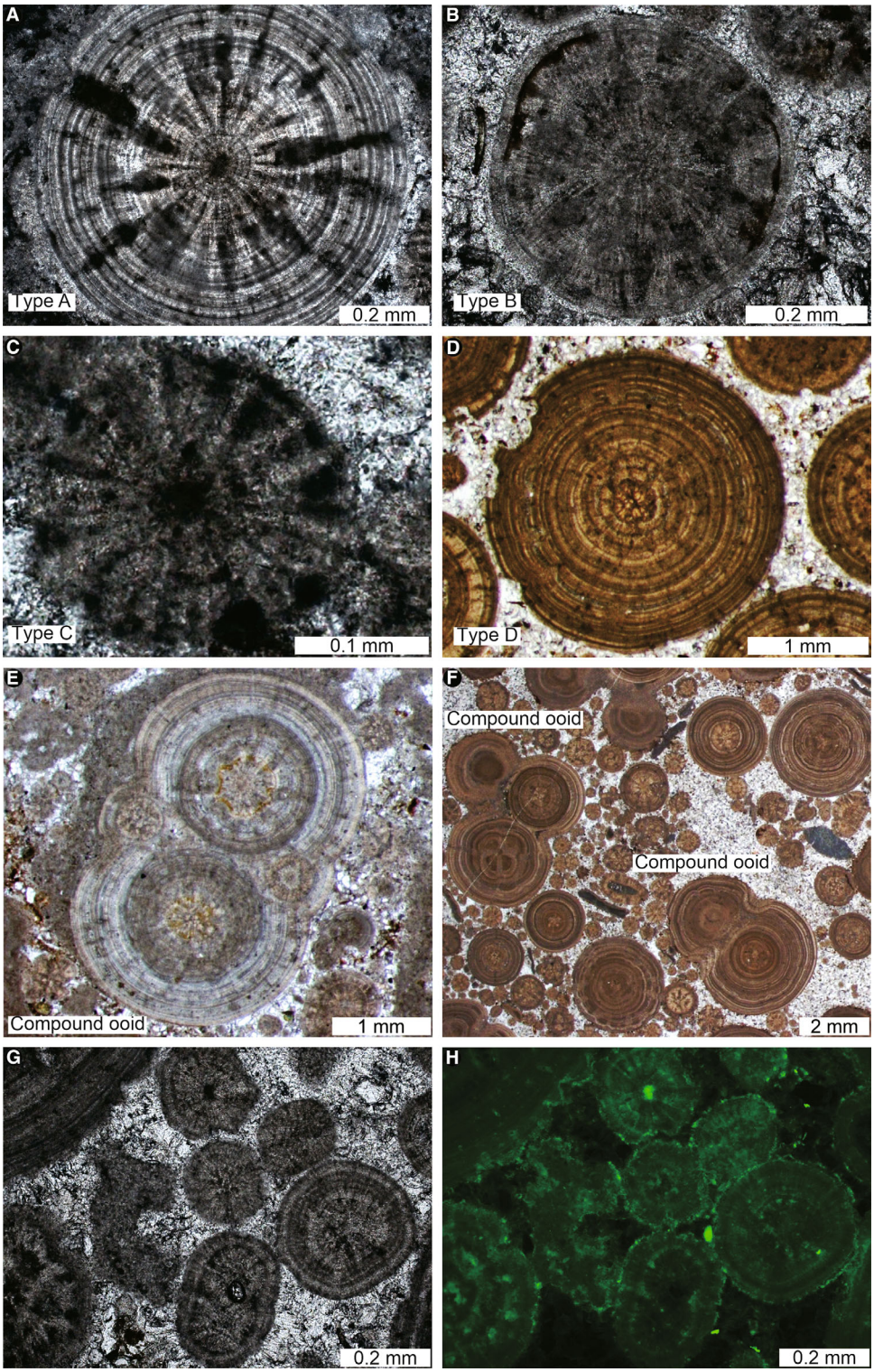

Fig. 3. Thin section images of the Early Triassic ooids from Germanic Basin. (A) Type A, characterized by co-occurring radial and tangential structures across their cortices. (B) Type B, with alternating radial and tangential features. (C) Type C, radial ooids showing indistinct laminae. (D) Type D, tangential ooids exhibiting indistinct radial features. (E) and (F) Compound ooids, formed by several ooids that have coalesced with one another during growth. (G) and (H) Same image under transmitted light (G) and fluorescence (H). Note that both radial and tangential cortices exhibit a strong green fluorescence, which is typically brighter in the darker radial segments and darker laminae.

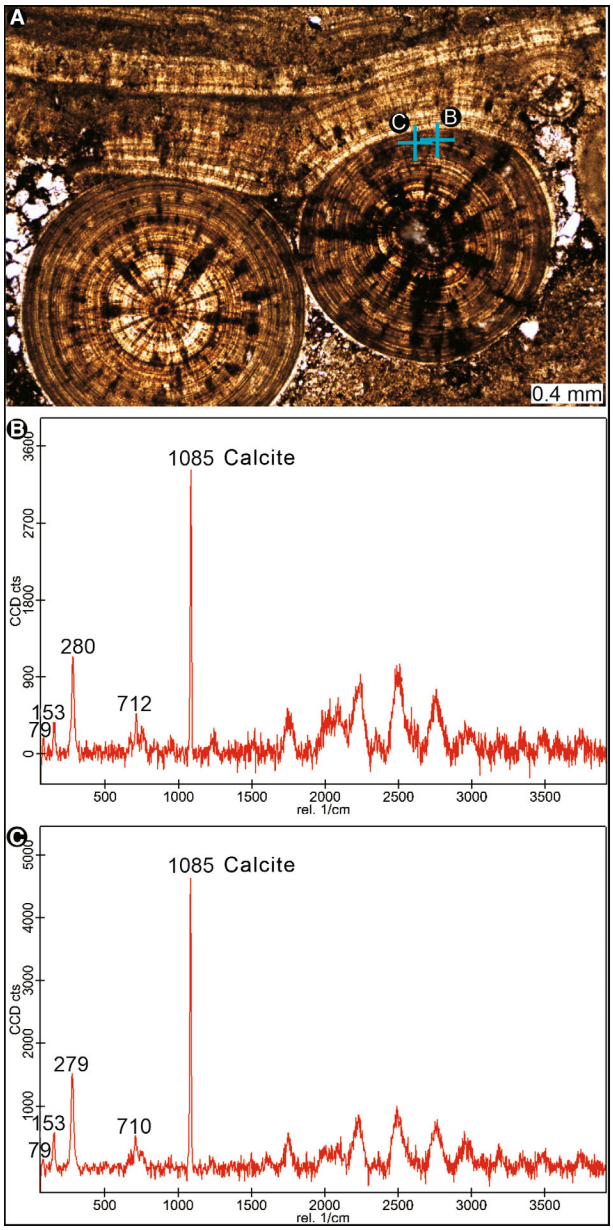

Fig. 4. Raman spectroscopy (single spectra) images of the Triassic ooids from Germanic Basin, showing that they are mainly composed of calcite. The unmarked peaks in (B) and (C) are attributed to fluorescence interference.

composed of calcite (Fig. 4). The dark and light radial segments display different contents of elements, for example, calcium (Ca) (Fig. 5A and B), iron (Fe) (Fig. 5A and C) and silicon (Si) (Fig. 5A and D), as indicated by μ-XRF. The matrix between ooids is typically enriched in Si, which is due to the presence of abundant quartz grains. At the same time, there is no petrographic or μ-XRF evidence for the presence of quartz grains in the centre of ooids.

Relationship between ooids and microbial crusts/stromatolites

The studied Germanic Basin ooids are often overlaid by laterally-continuous microbial crusts equivalent to the initial stage of stromatolites (Fig. 2C and D). Ooids and microbial crusts also alternate on a millimetre-scale (Fig. 6A). In other cases, microbial crusts completely envelop clusters of ooids (Fig. 6B), which was already described by Kalkowsky (1908) as 'ooid bags' (Ooid Beutel) and also observed by other researchers (Paul & Peryt, 2000; Paul *et al.*, 2011).

Furthermore, the microfabric of both ooid laminae and stromatolite laminae is almost identical, with laminae showing a characteristic internal palisade structure composed by thin crystals growing perpendicular to lamination (Fig. 6C and D). In addition, the microbial crusts also show structures equivalent to the radial and tangential structures of ooid cortices (Fig. 6E and F). Locally, truncation is observed between the ooid cortices and the overlying microbial crusts, but the microfabric of laminae remains equivalent (Fig. 6A).

Modern ooids from the Great Salt Lake

Morphology and composition

Great Salt Lake deposits contain abundant ooids and associated microbial crusts (Chidsey *et al.*, 2015; Vennin *et al.*, 2019) (Fig. 7A). The studied Great Salt Lake ooids range from 0.2 to 1.0 mm in diameter and are ellipsoidal to subspherical in shape (Figs 7 to 9). The nuclei of ooids are either micritic particles or detrital (quartz or feldspar) grains (Figs 7, 8C and 9A). Ooid cortices are aragonitic, as indicated by Raman spectroscopy (Fig. 8D to F).

Great Salt Lake ooids can be classified based on their cortex structures and include the same types as the Triassic deposits from the Germanic Basin (Fig. 7A to C, E to G). Type A ooids show co-occurring radial and tangential structures across their cortices (Fig. 7C). Type B ooids exhibit alternating radial and tangential features (Fig. 7A, B and E to G). Type C ooids are radial showing indistinct laminae (Fig. 7E). Type D ooids are tangential exhibiting indistinct radial features (Fig. 7E). Raman spectroscopy indicates different preferred orientations of aragonite crystals in radial and tangential parts of the cortices (Fig. 8D to F). FE-SEM shows that radial parts of the cortices consist of >50 μm long fan-shaped crystals. Tangential parts are formed by alternating laminae of radial crystals and smaller

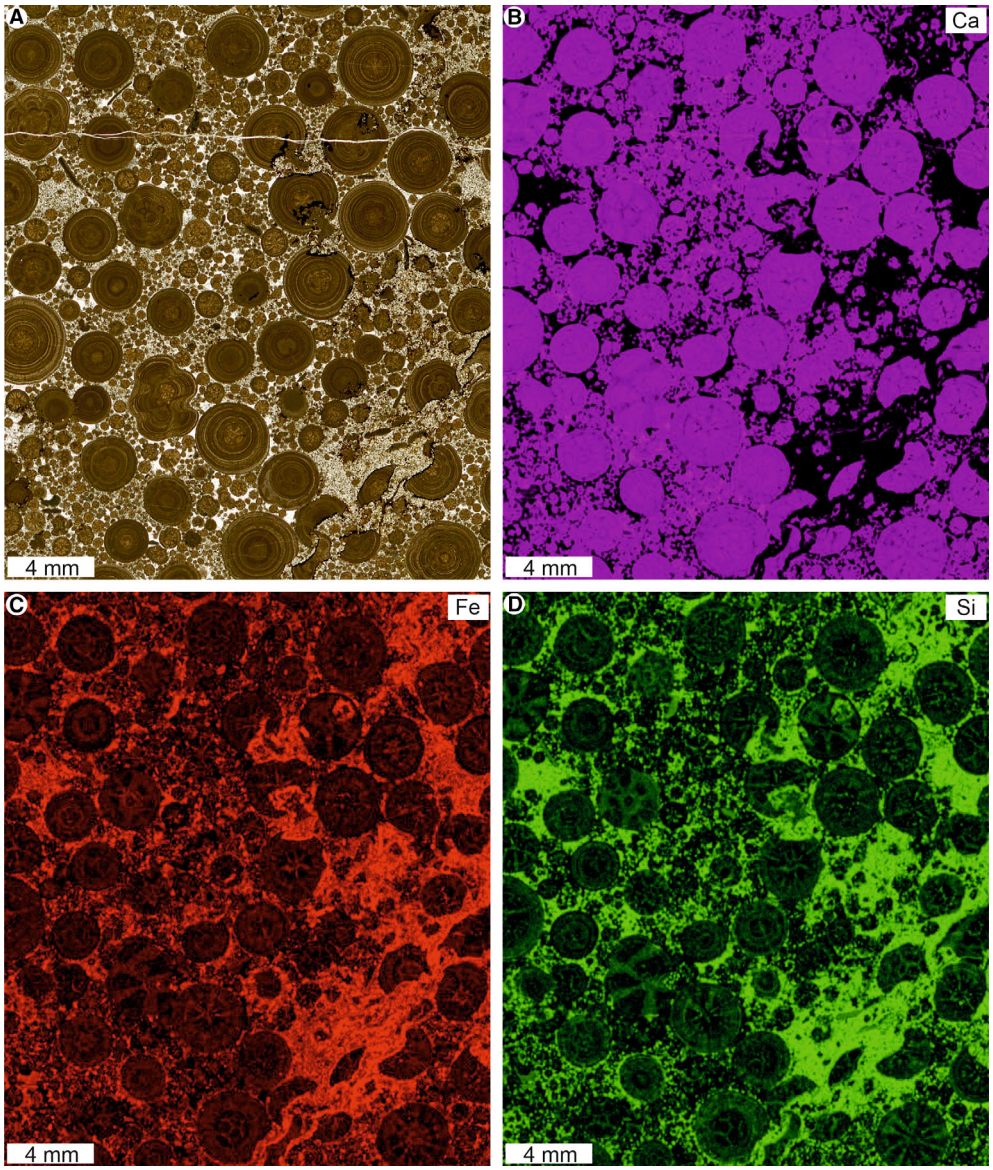

Fig. 5. Micro X-ray fluorescence (μ-XRF) images of the Triassic ooids from Germanic Basin. (A) Scan image (transmitted light). (B) Calcium (Ca) distribution. (C) Iron (Fe) distribution. (D) Silicon (Si) distribution.

(<5 μm) needles with irregular arrangement (Fig. 9). 'Compound ooids' are rarely observed.

Organic matter (OM) in ooids

Great Salt Lake ooids show significant internal differences in the intensity of green fluorescence (Fig. 7E to H). Tangential cortices have a brighter green fluorescence than those with radial structures and, in the radial ones, the dark radial segments show a brighter green fluorescence than the lighter segments (Fig. 7E to H). Occasionally, a very bright green rim is observed at the outer edge (Fig. 7E and F). Alcian blue staining, which indicates the presence of carboxylic groups in acidic polysaccharides, is stronger in tangential cortices than in radial ones (Fig. 7B).

Fluorescent dye calcein detects free Ca^{2+} in acidic OM, and the concentrations of free Ca^{2+} are reflected by fluorescence intensities with different colours (Reitner *et al.*, 1997). In Great Salt Lake ooids, from their outer edge to their inside, orange, yellow and green colours are observed (Fig. 7C and D), suggesting declining abundance of free Ca^{2+} and acidic OM, corresponding with a gradual increase in mineralization.

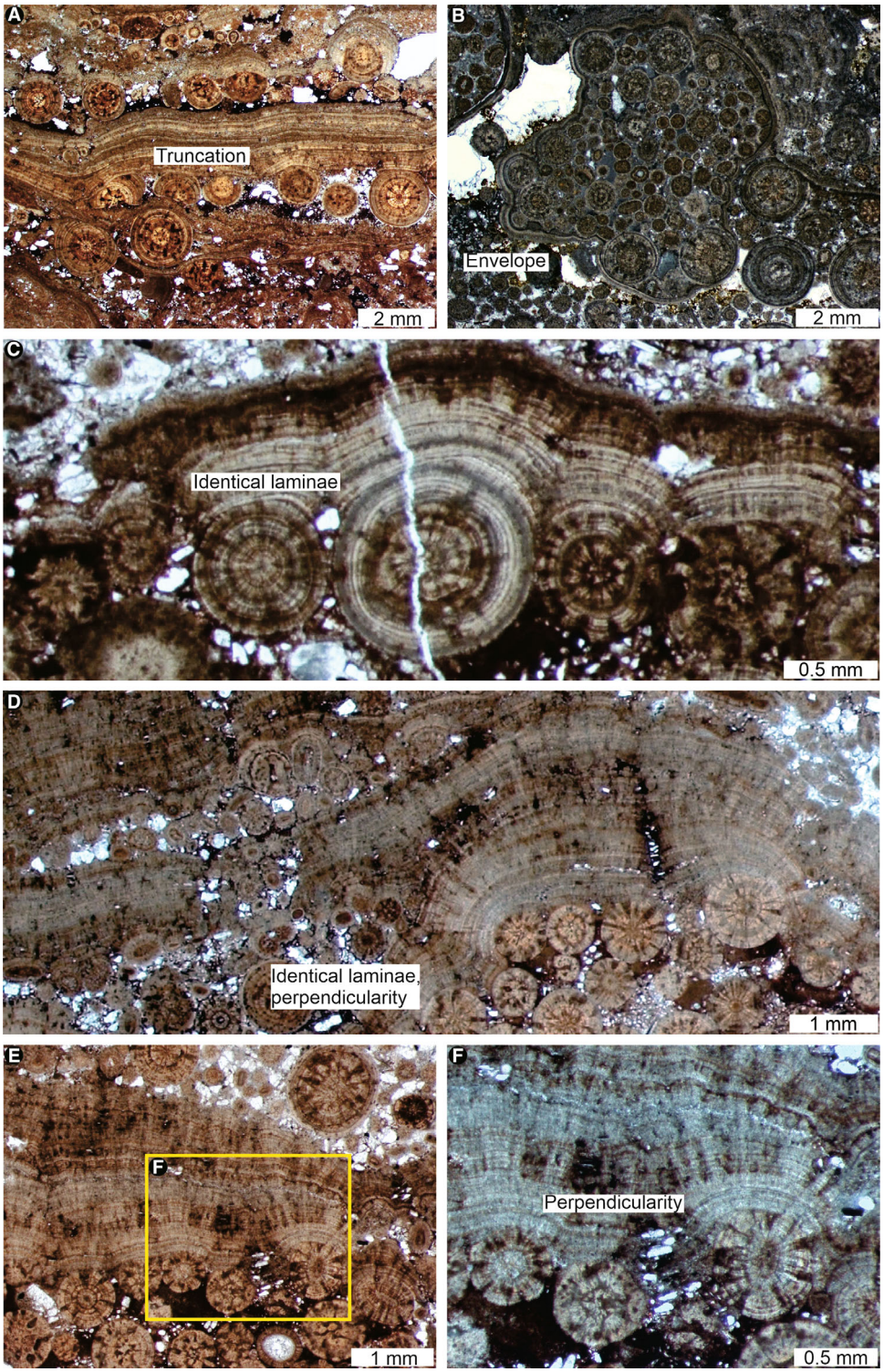

Fig. 6. Thin section images of the ooids and microbial crusts/stromatolites of the Early Triassic from Germanic Basin. (A) Ooids and microbial crusts alternate on a millimetre-scale. Truncation is observed between the ooid cortices and the overlying microbial crusts. (B) Microbial crusts completely envelop clusters of ooids. (C) and (D) The microfabric of both ooid laminae and stromatolite laminae is almost identical, with laminae showing a characteristic internal palisade structure composed by thin crystals growing perpendicular to lamination. (E) and (F) The microbial crusts also show structures equivalent to the radial and tangential structures of ooid cortices. The rectangle in (E) is magnified as (F).

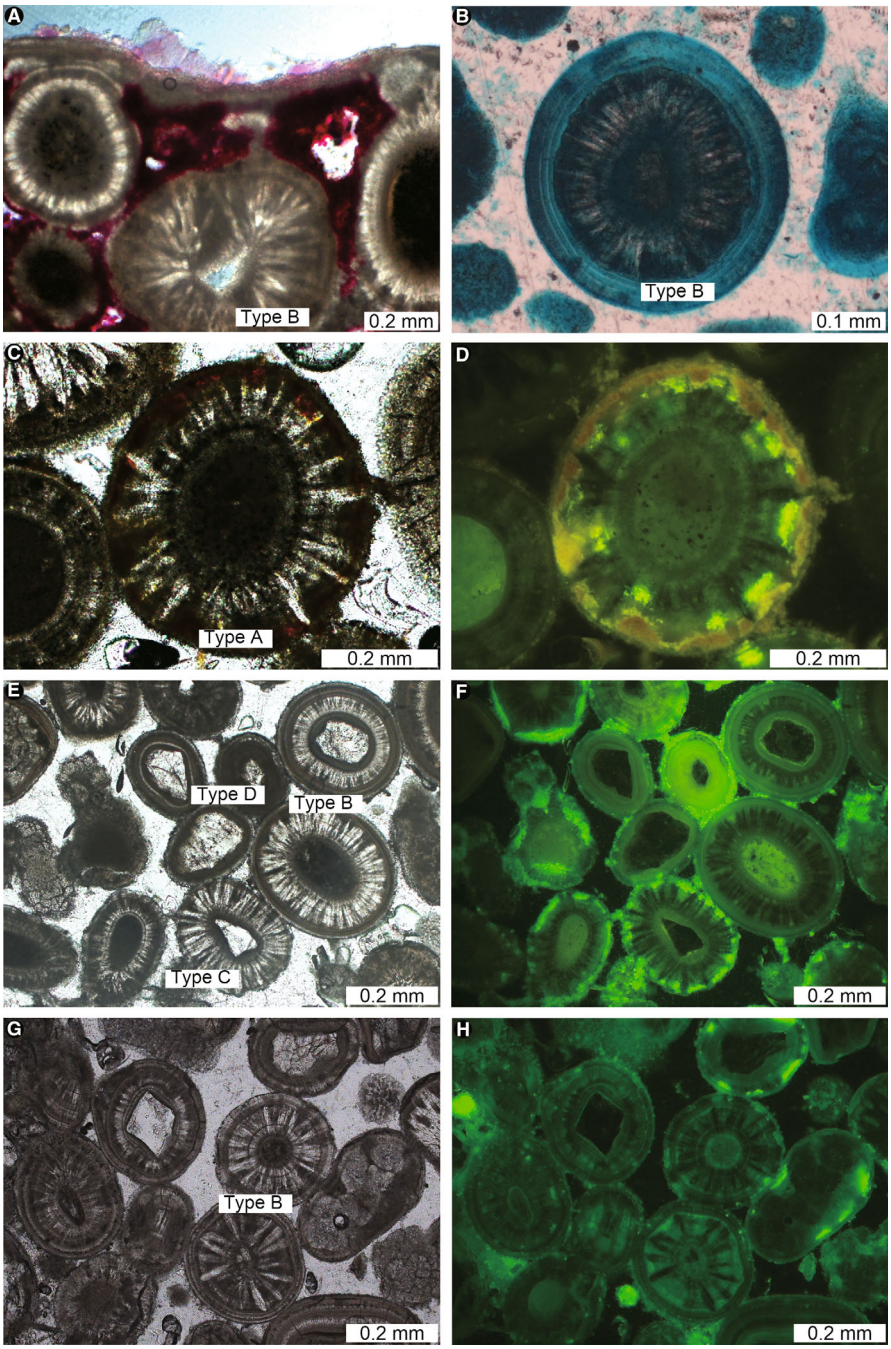

Fig. 7. Thin section images of the ooids and/or microbial crusts from Great Salt Lake. Note that their cortex structures are similar to those of the Triassic specimens. (A) Ooids, with cortices showing alternating radial and tangential features (Type B), which are overlaid by thin microbial crusts (basic fuchsin stain). (B) Type B ooid, with alternating radial and tangential features. Note that alcian blue staining is stronger in tangential cortices than that in radial ones. (C) Type A ooid, characterized by co-occurring radial and tangential structures across their cortices. (D) Same image as (C), under fluorescence. Note that, from the outer edge to the inside, orange, yellow and green colours are observed, suggesting declining abundance of free Ca^{2+} and acidic OM, corresponding with a gradual increase in mineralization. (E) and (G) Ooids corresponding to Type B (alternating radial and tangential features in the cortex), Type C (radial ooids showing indistinct laminae) and Type D (tangential ooids exhibiting indistinct radial features). (F) and (H) Same images as (E) and (G), under fluorescence. Significant internal differences in the intensity of fluorescence are shown. Tangential cortices have a brighter green fluorescence than those with radial structures. In the radial ones, the dark radial segments show a brighter green fluorescence than the lighter segments. Occasionally, a very bright green rim is observed at the outer edge.

DISCUSSION

Comparison of the Germanic Basin and Great Salt Lake ooids

The Germanic Basin and Great Salt Lake ooids have some obvious differences, mainly size (Germanic Basin ooids are typically much larger than Great Salt Lake ooids), shape (Germanic Basin ooids are mainly spherical while Great Salt Lake ooids are predominantly ellipsoidal) and composition (Germanic Basin ooids are mainly composed of calcite while Great Salt Lake ooids are predominantly aragonite) (Figs 3, 4, 7 and 8). The size of Germanic Basin ooids is generally larger than that of Great Salt Lake ooids, perhaps attributed to the water geochemistry during the Permian–Triassic critical juncture (Li *et al.*, 2021). Because the environment is very dynamic in the Germanic Basin, transportation after formation of the Germanic Basin ooids also supports their high sphericity. Meanwhile, the formation of Great Salt Lake ooids is perhaps still an active process (Anderson *et al.*, 2013).

At the same time, Germanic Basin and Great Salt Lake ooids share remarkable similarities, which is why they have been compared previously (Käsbohrer & Kuss, 2019; Pei, 2022). For instance, Germanic Basin and Great Salt Lake ooids display the same types of cortices, that is, cortices with radial structure (Type C), cortices with tangential structure (Type D) and cortices with either a mixture or an alternation of both structures (Type A and B, respectively) (Figs 3 and 7). Besides, ooids from both settings have micritic particles as nuclei and are rich in radial features (Figs 3 and 7). Fluorescence microscopy indicates the presence of OM in ooids from the Germanic Basin (Fig. 3G and H) and the Great Salt Lake (Fig. 7). However, OM contents seem to be much lower in the case of Germanic Basin ooids, which is likely due to degradation through geological time.

Ooid types similar to those from the Germanic Basin and Great Salt Lake have been observed in modern hypersaline environments (Friedmann *et al.*, 1973, 1985; Loreau & Purser, 1973; Krumbein & Cohen, 1974; Krumbein, 1983; Strasser, 1986; Gerdes *et al.*, 1994, 2000; Hubert *et al.*, 2018; Suarez-Gonzalez & Reitner, 2021). In agreement with the geological settings and water chemistry, ooids from both deposits investigated herein are supposed to have formed under hypersaline conditions as well (Paul & Peryt, 2000; Chidsey *et al.*, 2015; Käsbohrer & Kuss, 2019).

Formation of ooids statically versus dynamically

Modern ooids from the Bahamas demonstrate that ooids from agitated environments are trapped and fused together as one of the main sources of sedimentary grains in stromatolites (Macintyre *et al.*, 2000; Reid *et al.*, 2000). The presence of abundant sedimentary structures (for example, cross-bedding, climbing ripples and wave ripples) and abundant detrital (mainly quartz) grains in the Germanic Basin and Great Salt Lake deposits indicate reworking and transportation processes (e.g. Reitner *et al.*, 1997; Paul & Peryt, 2000; Käsbohrer & Kuss, 2019) (Figs 4 and 6). Yet, various lines of evidence suggest that ooids from both deposits were not formed dynamically during transportation. For instance, quartz grains are abundant constituents of the deposits, but almost never or partially form the nuclei of the ooids (Figs 3 to 9). Instead, the nuclei of ooids typically consist of small micritic particles, which are themselves rare constituents of the oolitic deposits. Furthermore, the Germanic Basin deposits contain abundant ‘compound ooids’ consisting of ooids that coalesced with one another during growth, which is inconsistent with growth through constant motion as bed-load or in suspension. These features (micritic nuclei in detrital matrix and cortex coalescence) have recently been shown as characteristic of modern ooids growing *in situ* within microbial mats (Suarez-Gonzalez & Reitner, 2021). At the same time, ooids and microbial crusts are closely related, and their microstructures are commonly identical, indicating that similar processes were involved in their formation (for example, Figs 6C to F and 7A). Taken together, the observed features suggest that these ooids developed statically (perhaps even within microbial mats) (e.g. O’Reilly *et al.*, 2017; Mariotti *et al.*, 2018; Anderson *et al.*, 2020), rather than formed around transported grains in agitated environments (e.g. Duguid *et al.*, 2010; Trower *et al.*, 2018).

Organic influence on ooid formation

Abundant OM within Great Salt Lake ooids (Fig. 7B and E to H), as well as increasing OM contents associated with decreasing mineralization degrees from the nuclei towards to the outer edge of ooids (Fig. 7C and D), may indicate a relationship between OM and carbonate formation.

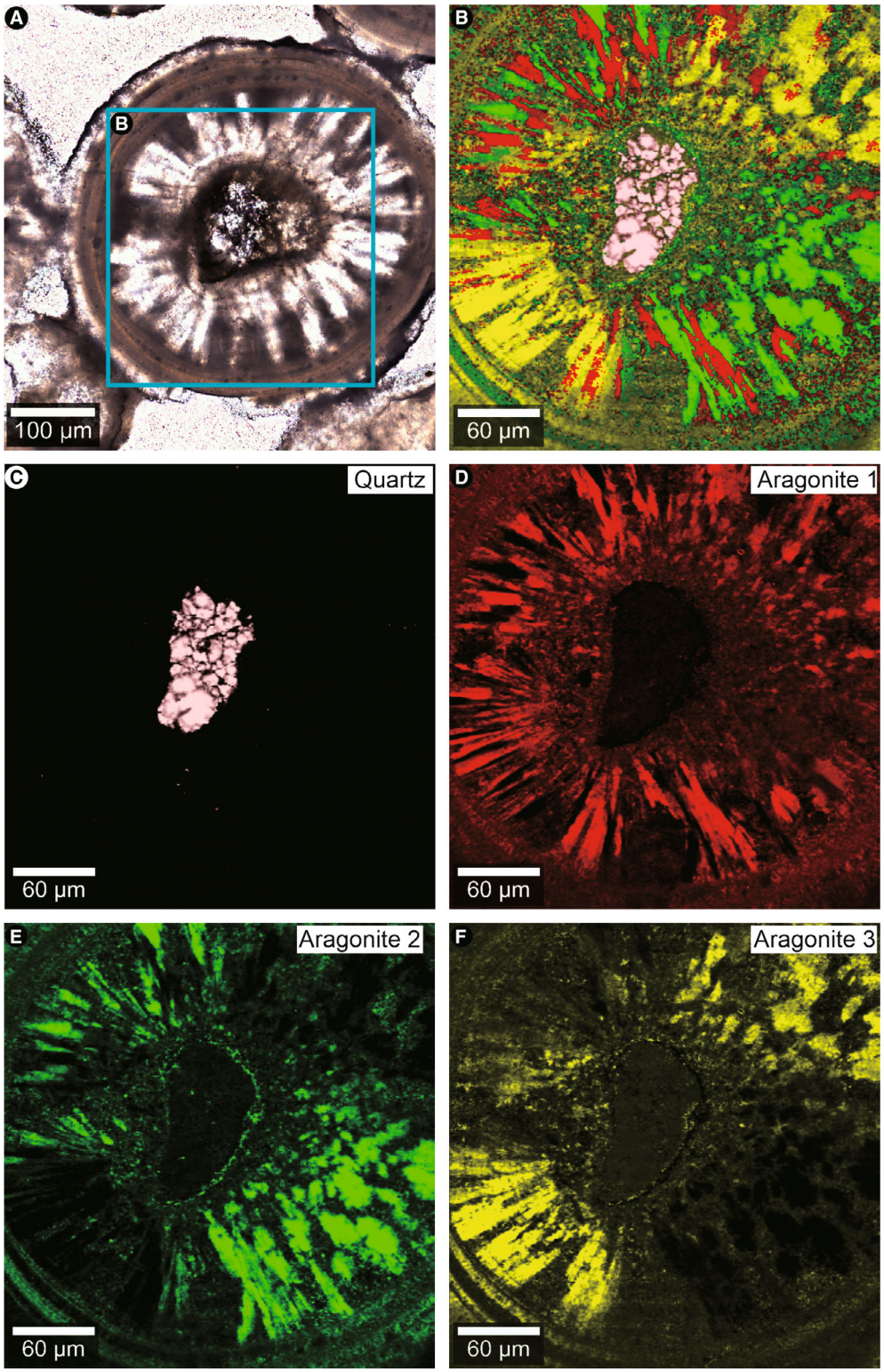

Fig. 8. Raman spectral images of modern ooids from Great Salt Lake. (A) Thin section image (transmitted light). (B) Combined image. (C) Quartz as the core. (D) to (F) Different preferred orientations of aragonite crystals. The rectangle in (A) is magnified as (B).

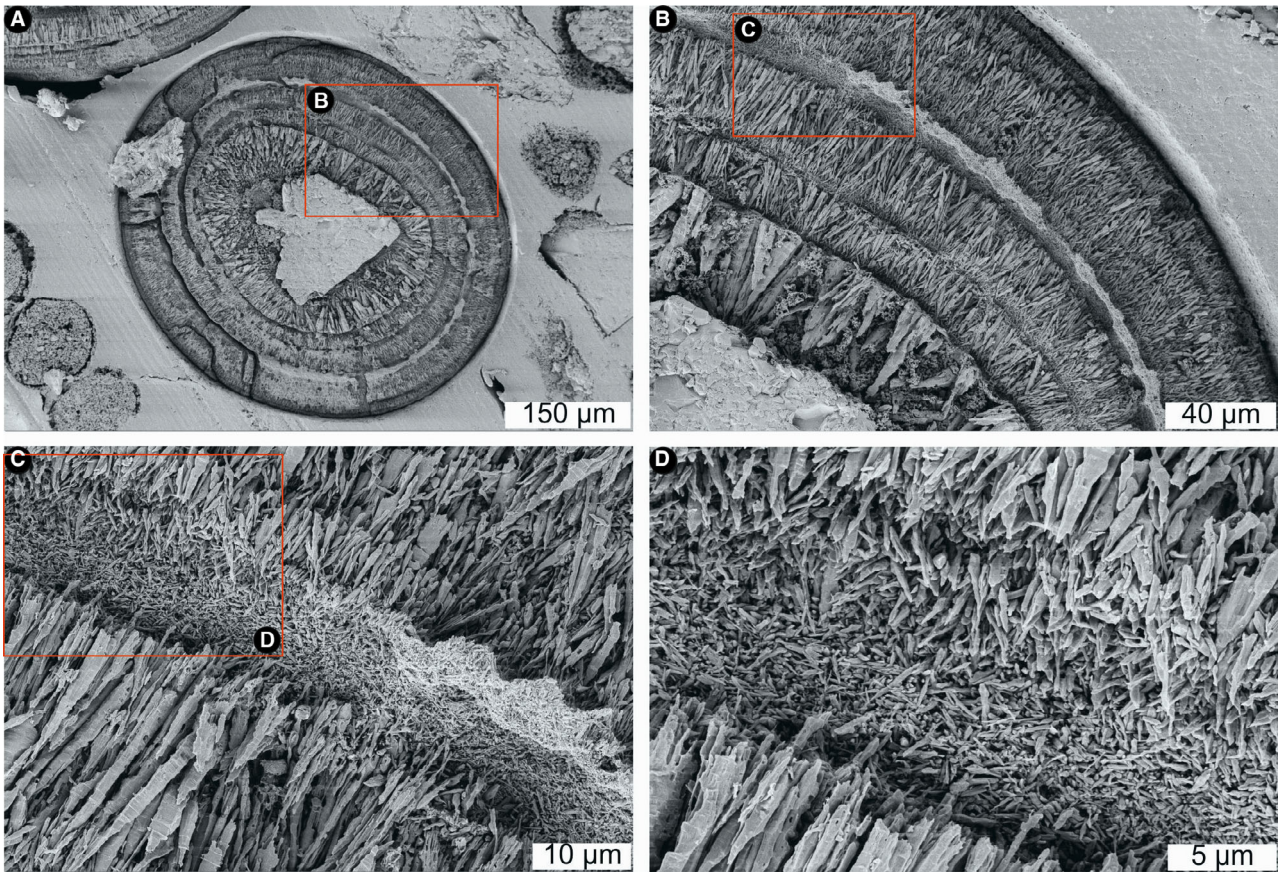

Fig. 9. Field emission scanning electron microscopy (FE-SEM) images of modern ooids from Great Salt Lake. (A) Type B ooids exhibit alternating radial and tangential features. (B) to (D) Radial parts of the ooid cortices consist of >50 μm long fan-shaped crystals. Tangential parts are formed by alternating laminae of radial crystals and smaller (<5 μm) needles with irregular arrangement. The rectangle in (A) is magnified as (B). The rectangle in (B) is magnified as (C). The rectangle in (C) is magnified as (D).

In the case of Germanic Basin ooids, the possible relationship between OM and carbonate minerals is less obvious, likely because OM has been degraded. However, as argued before, microbial crusts in the Germanic Basin deposits typically represent a continuation of the microfabric of the ooid cortices (for example, Fig. 6C to F), suggesting similar formation processes. Notably, Kalkowsky (1908), in the same ground-breaking study where he coined the term 'stromatolite', already used this to argue for an organic influence on the origin of ooids in the Germanic Basin, stating that: "if somebody insists on the inorganic genesis of ooids, he will, however, never find a good explanation for [the fact that] (…) ooids often form the initiating stage of stromatolites" (translated by Krumbein, 1983; Paul *et al.*, 2011), which underlines the great value and continuing impact of this observation-based research.

Besides, Lincoln *et al.* (2022) has demonstrated that microbial sulphur cycling likely drives the formation of radial cortices in Great Salt Lake ooids. Microbial processes might also have been involved in the formation of other ancient ooids, which are very similar to the Triassic examples studied herein (Granier & Lapointe, 2021, 2022). Actually, the organic origin of these crusts with fibrous–palisade microstructure is hard to establish, and they have been previously interpreted as mostly inorganic, although some microbial influence was not ruled out (Paul & Peryt, 2000). It is true that, in modern environments, similar fibrous microfabrics and crusts occur during moments of environmental increase in $CaCO_3$ supersaturation, but typically within microbial communities (e.g. Suarez-Gonzalez & Reitner, 2021), and they have also been observed within fossil microbialites (Camoin *et al.*, 1997; Kirkham & Tucker, 2018).

Possible ooid formation processes

Various factors have been traditionally proposed for explaining differences in the cortex structures of ooids, mainly dealing with different environmental conditions (Strasser, 1986). The results presented herein underline the general significance of OM in ooid formation, raising the intriguing possibility that the internal structure of ooids may be controlled by the chemical nature of the involved OM. One important function of microbial EPS is the inhibition of mineral precipitation (e.g. Decho, 2010). At the same time, however, OM can function as a nucleation site for mineralization ('Organomineralization': Mitterer, 1968; Suess & Fütterer, 1972; Ferguson *et al.*, 1978; Trichet & Défarge, 1995; Reitner *et al.*, 1995a,b, 1997; Reitner, 2004). The observed different intensities of alcian blue staining [indicative for the presence of carboxylic groups (COO^-) in acidic polysaccharides] and green fluorescence (likely indicative for the content of OM) between tangential and radial cortices in Great Salt Lake ooids (Fig. 7B, F and H) suggest potential differences of OM in forming both cortices. Potentially degraded OM is more involved in forming radial cortices while fresher EPS is more related with tangential cortices (Fig. 10). However, further

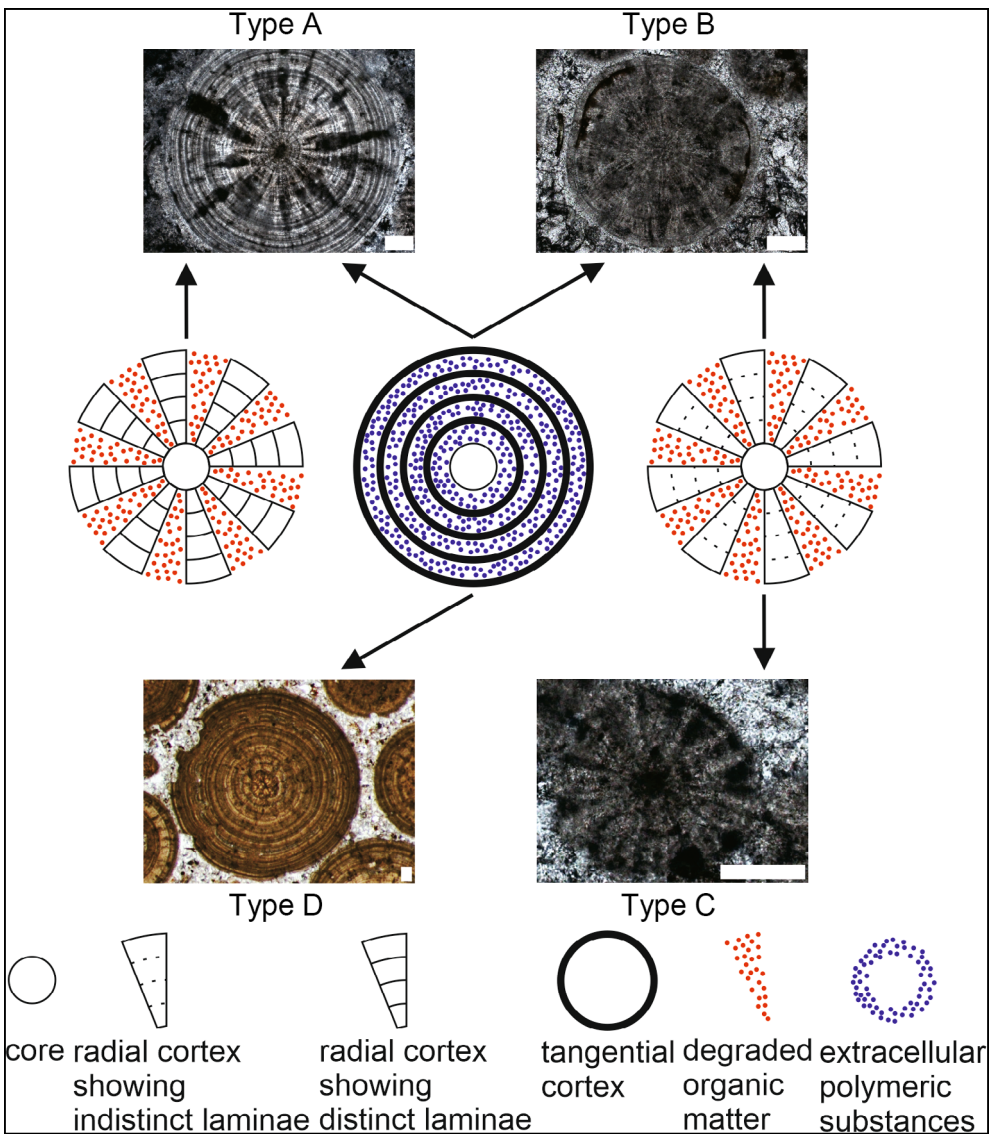

Fig. 10. Extracellular polymeric substances (EPS) and degraded organic matter (OM) shape four types of ooids. Potentially degraded OM is more involved in forming radial cortices while fresher EPS is more related with tangential cortices. All scale bars represent 0.1 mm.

research on OM associated with different types of ooids is needed.

CONCLUSIONS

This study investigated ooids in deposits from the Great Salt Lake and Germanic Basin, two world-famous geobiological sites. Ooids in both localities display extreme similarities in their internal microstructures, suggesting that they could have been formed by similar processes. The micritic ooid nuclei, the common presence of 'compound ooids' as well as identical characteristics of ooid laminae and overlaid microbial crusts are all supportive of static growth. Organic matter (OM) is present in interspaces between radial and tangential ooid cortices and becomes more abundant towards the outer edge in the case of radial ooids. Together, these features strongly indicate that acidic OM played a key-role in the formation of ooids. This is additionally supported by the close association of ooids and microbial crusts in the Germanic Basin deposits, since the latter typically form through mineral precipitation associated with OM.

ACKNOWLEDGEMENTS

We thank Associate Editor Stephen Lokier and two anonymous reviewers for their constructive comments. We also acknowledge Chief Editor Gabriela Mángano for the guidance through the editorial process. Axel Hackmann and Wolfgang Dröse are thanked for assistance in the lab. This study was financially supported by the Göttingen Academy of Sciences and Humanities and by the research project PID2022-136717NB-I00 of the Government of Spain. YP gratefully received financial support from the China Scholarship Council (CSC), the University of Tübingen (Teach@Tübingen Fellowship) and China Postdoctoral Science Foundation (2023 M743291). PSG acknowledges funding by a postdoctoral "Humboldt Research Fellowship" of the Alexander von Humboldt Foundation. Open Access funding enabled and organized by Projekt DEAL.

DATA AVAILABILITY STATEMENT

The data that support the findings of this study are available from the corresponding author upon reasonable request.

REFERENCES

Anderson, R.P., **Bird, J.T.**, **Meneske, M.**, **Stefurak, E.J.**, **Berelson, W.**, **Petryshyn, V.A.**, **Shapiro, R.S.**, **Sessions, A.L.**, **Tripati, A.** and **Corsetti, F.A.** (2013) Ooid formation in the Great Salt Lake, Utah: Insights from clumped isotope paleothermometry. *AGU Fall Meeting Abstracts*, PP23A-1941.

Anderson, N.T., **Cowan, C.A.** and **Bergmann, K.D.** (2020) A case for the growth of ancient ooids within the sediment pile. *J. Sediment. Res.*, **90**, 843–854.

Binsteiner, A., **Prichystal, A.**, **Wessely, G.**, **Antl-Weiser, W.** and **Kern, A.** (2008) Neue Untersuchungen zum Kalkoolith der Venus von Willendorf. *Mitteilungen der Anthropologischen Gesellschaft in Wien*, **138**, 23–35.

Brehm, U., **Krumbein, W.E.** and **Palinska, K.A.** (2006) Biomicrospheres generate ooids in the laboratory. *Geomicrobiol. J.*, **23**, 545–550.

Brückmann, F.E. (1721) Specimen physicum exhibens historam naturalem Oolithi, *Helmestadii Salomonis Schnorri*, pp. 28.

Burne, R.V., **Eade, J.C.** and **Paul, J.** (2012) The natural history of ooliths: Franz Ernst Brückmann's treatise of 1721 and its signifcance for the understanding of oolites. *Hallesches Jahrbuch für Geowissenschaften*, **34**, 93–114.

Camoin, G., **Casanova, J.**, **Rouchy, J.-M.**, **Blanc-Valleron, M.-M.** and **Deconinck, J.-F.** (1997) Environmental controls on perennial and ephemeral carbonate lakes: The central palaeo-Andean Basin of Bolivia during Late Cretaceous to early Tertiary times. *Sediment. Geol.*, **113**, 1–26.

Chidsey, T.C., **Vanden Berg, M.D.** and **Eby, D.E.** (2015) Petrography and characterization of microbial carbonates and associated facies from modern Great Salt Lake and Uinta Basin's Eocene Green River Formation in Utah, USA. In: *Microbial Carbonates in Space and Time: Implications for Global Exploration and Production* (Eds Bosence, D.W.J., Gibbons, K.A., Le Heron, D.P., Morgan, W.A., Pritchard, T. and Vining, B.A.), *Geological Society, London, Special Publications*, **418**, 261–286.

Davies, P.J., **Bubela, B.** and **Ferguson, J.** (1978) The formation of ooids. *Sedimentology*, **25**, 703–730.

Decho, A.W. (2010) Overview of biopolymer-induced mineralization: What goes on in biofilms? *Ecol. Eng.*, **36**, 137–144.

Decho, A.W. and **Gutierrez, T.** (2017) Microbial extracellular polymeric substances (EPSs) in ocean systems. *Front. Microbiol.*, **8**, 922.

Diaz, M.R. and **Eberli, G.P.** (2019) Decoding the mechanism of formation in marine ooids: A review. *Earth-Sci. Rev.*, **190**, 536–556.

Diaz, M.R., **Swart, P.K.**, **Eberli, G.P.**, **Oehlert, A.M.**, **Devlin, Q.**, **Saeid, A.** and **Altabet, M.A.** (2015) Geochemical evidence of microbial activity within ooids. *Sedimentology*, **62**, 2090–2112.

Diaz, M.R., **Eberli, G.P.**, **Blackwelder, P.**, **Phillips, B.** and **Swart, P.K.** (2017) Microbially mediated organomineralization in the formation of ooids. *Geology*, **45**, 771–774.

Duguid, S.M.A., **Kyser, T.K.**, **James, N.P.** and **Rankey, E.C.** (2010) Microbes and ooids. *J. Sediment. Res.*, **80**, 236–251.

Ferguson, J., **Bubela, B.** and **Davies, P.J.** (1978) Synthesis and possible mechanism of formation of radial carbonate ooids. *Chem. Geol.*, **22**, 285–308.

Flannery, D.T., **Allwood, A.C.**, **Hodyss, R.**, **Summons, R.E.**, **Tuite, M.**, **Walter, M.R.** and **Williford, K.H.** (2019) Microbially influenced formation of Neoarchean ooids. *Geobiology*, **17**, 151–160.

Flemming, H.-C. (2016) EPS—then and now. *Microorganisms*, **4**, 41.

Flemming, H.-C. and **Wingender, J.** (2010) The biofilm matrix. *Nat. Rev. Microbiol.*, **8**, 623–633.

Flemming, H.-C., **Neu, T.R.** and **Wozniak, D.J.** (2007) The EPS matrix: The "house of biofilm bells". *J. Bacteriol.*, **189**, 7945–7947.

Flügel, E. (2010) *Microfacies of Carbonate Rocks*. Springer, Heidelberg, Dordrecht, London, New York.

Friedmann, G.M., **Amiel, A.J.**, **Braun, M.** and **Miller, D.S.** (1973) Generation of carbonate particles and laminites in algal mats—example from sea-marginal hypersaline pool, Gulf of Aqaba, Red Sea. *Am. Assoc. Petrol. Geol. Bull.*, **57**, 541–557.

Friedmann, G.M., **Sneh, A.** and **Owen, R.W.** (1985) The Ras Muhammad Pool: Implications for the Gavish Sabkha. In: *Hypersaline Ecosystems—The Gavish Sabkha* (Eds Krumbein, W.E. and Friedman, G.M.), pp. 218–237. Springer, Berlin.

Gerdes, G., **Dunajtschik-Piewak, K.**, **Riege, H.**, **Taher, A.G.**, **Krumbein, W.E.** and **Reineck, H.-E.** (1994) Structural diversity of biogenic carbonate particles in microbial mats. *Sedimentology*, **41**, 1273–1294.

Gerdes, G., **Krumbein, W.E.** and **Noffke, N.** (2000) Evaporite microbial sediments. In: *Microbial Sediments* (Eds Riding, R.E. and Awramik, S.M.), pp. 196–208. Springer, Berlin.

Granier, B.R.C. and **Lapointe, P.** (2021) The Kalkowsky Project – Chapter I. Ooid – stromatoid relationship in a stromatolite from the Maiz Gordo Fm (Argentina). *Carnets Geol.*, **21**, 193–201.

Granier, B.R.C. and **Lapointe, P.** (2022) The Kalkowsky Project – Chapter II. Wobbly ooids in a stromatolite from the Yacoraite Formation (Argentina). *Carnets Geol.*, **22**, 111–117.

Hicks, J.D. and **Matthaei, E.** (1958) A selective fluorescence stain for mucin. *J. Pathol. Bacteriol.*, **75**, 473–476.

Hubert, H.L., **Rankey, E.C.** and **Omelon, C.** (2018) Organic matter, textures, and pore attributes of hypersaline lacustrine microbial deposits (Holocene, Bahamas). *J. Sediment. Res.*, **88**, 827–849.

Illing, L.V. (1954) Bahaman calcareous sands. *Bull. Am. Assoc. Petrol. Geol.*, **38**, 1–95.

Ingalls, M., **Frantz, C.M.**, **Snell, K.E.** and **Trower, E.J.** (2020) Carbonate facies-specific stable isotope data record climate, hydrology, and microbial communities in Great Salt Lake, UT. *Geobiology*, **18**, 566–593.

Kalkowsky, E. (1908) Oolith und Stromatolith im norddeutschen Buntsandstein. *Zeitschrift der Deutschen Geologischen Gesellschaft Band*, **60**, 68–125.

Käsbohrer, F. and **Kuss, J.** (2019) Sedimentpetrographische Untersuchungen der Calvörde-Formation (Unterer Buntsandstein, Untertrias). *Hallesches Jahrbuch für Geowissenschaften*, **42**, 1–24.

Käsbohrer, F. and **Kuss, J.** (2021) Lower Triassic (Induan) stromatolites and oolites of the Bernburg Formation revisited – microfacies and palaeoenvironment of lacustrine carbonates in Central Germany. *Facies*, **67**, 11.

Kirkham, A. and **Tucker, M.E.** (2018) Thrombolites, spherulites and fibrous crusts (Holkerian, Purbeckian, Aptian): Context, fabrics and origins. *Sediment. Geol.*, **374**, 69–84.

Krumbein, W.E. (1983) Stromatolites – The challenge of a term in space and time. *Precambrian Res.*, **20**, 493–531.

Krumbein, W.E. and **Cohen, Y.** (1974) Biogene, klastische und evaporitische Sedimentation in einem mesothermen monomiktischen ufernahen See (Golf von Aqaba). *Geologische Rundschau*, **63**, 1035–1065.

Li, F., **Yan, J.**, **Chen, Z.-Q.**, **Ogg, J.G.**, **Tian, L.**, **Korngreen, D.**, **Liu, K.**, **Ma, Z.** and **Woods, A.D.** (2015) Global oolite deposits across the Permian–Triassic boundary: A synthesis and implications for palaeoceanography immediately after the end-Permian biocrisis. *Earth-Sci. Rev.*, **149**, 163–180.

Li, X., **Trower, E.J.**, **Lehrmann, D.J.**, **Minzoni, M.**, **Kelley, B.M.**, **Schaal, E.K.**, **Altiner, D.**, **Yu, M.** and **Payne, J.L.** (2021) Implications of giant ooids for the carbonate chemistry of Early Triassic seawater. *Geology*, **49**, 156–161.

Lincoln, T.A., **Webb, S.M.**, **Present, T.M.**, **Magyar, J.S.** and **Trower, E.J.** (2022) Microbial activity and neomorphism influence the composition and microfabric of ooids from Great Salt Lake, UT. *Sediment. Rec.*, **20**.

Lokier, S.W. and **Al Junaibi, M.** (2016) The petrographic description of carbonate facies: Are we all speaking the same language? *Sedimentology*, **63**, 1843–1885.

Loreau, J.P. and **Purser, B.H.** (1973) Distribution and ultrastructure of Holocene ooids in the Persian Gulf. In: *The Persian Gulf* (Ed Purser, B.H.), pp. 279–328. Springer, Berlin.

Macintyre, I.G., **Prufert-Bebout, L.** and **Reid, R.P.** (2000) The role of endolithic cyanobacteria in the formation of lithified laminae in Bahamian stromatolites. *Sedimentology*, **47**, 915–921.

Mariotti, G., **Pruss, S.**, **Summons, R.**, **Newman, S.** and **Bosak, T.** (2018) Contribution of benthic processes to the growth of ooids on a low-energy shore in Cat Island, The Bahamas. *Minerals*, **8**, 252.

Mitterer, R.M. (1968) Amino acid composition of organic matrix in calcareous oolites. *Science*, **162**, 1498–1499.

Neu, T.R. and **Lawrence, J.R.** (2010) Chapter 37 – Extracellular polymeric substances in microbial biofilms. In: *Microbial Glycobiology* (Eds Holst, O., Brennan, P.J., Itzstein, M.V. and Moran, A.P.), pp. 733–758. Academic Press, Amsterdam.

O'Reilly, S.S., **Mariotti, G.**, **Winter, A.R.**, **Newman, S.A.**, **Matys, E.D.**, **McDermott, F.**, **Pruss, S.B.**, **Bosak, T.**, **Summons, R.E.** and **Klepac-Ceraj, V.** (2017) Molecular biosignatures reveal common benthic microbial sources of organic matter in ooids and grapestones from Pigeon Cay, The Bahamas. *Geobiology*, **15**, 112–130.

Oviatt, C.G., **Thompson, R.S.**, **Kaufman, D.S.**, **Bright, J.** and **Forester, R.M.** (1999) Reinterpretation of the Burmester Core, Bonneville Basin, Utah. *Quatern. Res.*, **52**, 180–184.

Paul, J. and **Peryt, T.M.** (2000) Kalkowsky's stromatolites revisited (Lower Triassic Buntsandstein, Harz Mountains, Germany). *Palaeogeogr. Palaeoclimatol. Palaeoecol.*, **161**, 435–458.

Paul, J., **Peryt, T.M.** and **Burne, R.V.** (2011) Kalkowsky's stromatolites and oolites (Lower Buntsandstein, Northern Germany). In: *Advances in Stromatolite Geobiology* (Eds Reitner, J., Quéric, N.-V. and Arp, G.), pp. 13–28. Springer, Berlin.

Pei, Y. (2022) *A Geobiological Approach to Carbonate Factories and Ecosystem Changes Across the Permian–Triassic Boundary*. PhD Thesis. Georg-August-Universität, Göttingen.

Plée, K., **Ariztegui, D.**, **Martini, R.** and **Davaud, E.** (2008) Unravelling the microbial role in ooid formation—Results of an in situ experiment in modern freshwater Lake Geneva in Switzerland. *Geobiology*, **6**, 341–350.

Reid, R.P., **Visscher, P.T.**, **Decho, A.W.**, **Stolz, J.F.**, **Bebout, B.M.**, **Dupraz, C.**, **Macintyre, I.G.**, **Paerl, H.W.**, **Pinckney, J.L.**, **Prufert-Bebout, L.**, **Steppe, T.F.** and **DesMarais, D.J.**

(2000) The role of microbes in accretion, lamination and early lithification of modern marine stromatolites. *Nature*, **406**, 989–992.

Reitner, J. (1993) Modern cryptic microbialite/metazoan facies from Lizard Island (Great Barrier Reef, Australia) formation and concepts. *Facies*, **29**, 3–39.

Reitner, J. (2004) Organomineralization: A clue to the understanding of meteorite-related "Bacteria-shaped" carbonate particles. In: *Origins* (Ed Seckbach, J.), pp. 195–212. Kluwer Academic Publishers, Dordrecht.

Reitner, J., **Gautret, P.**, **Marin, F.** and **Neuweiler, F.** (1995a) Automicrites in a modern microbialite-Formation model via organic matrices (Lizard Island, Great Barrier Reef, Australia). *Bulletin de l'Institut océanographique de Monaco*, **14**, 237–263.

Reitner, J., **Neuweiler, F.** and **Gautret, P.** (1995b) Modern and fossil automicrites: implications formud mound genesis. In: *Mud Mounds: A Polygenetic Spectrum of Fine-Grained Carbonate Buildups* (Eds Flajs, G., Vigener, M., Keupp, H., Meischner, D., Neuweiler, F., Paul, J., Reitner, J., Warnke, K., Weller, H., Dingle, P., Hensen, C., Schäfer, P., Gautret, P., Leinfelder, R.R., Hüssner, H. and Kaufmann, B.), *Facies*, **32**, 1–69.

Reitner, J., **Arp, G.**, **Thiel, V.**, **Gautret, P.**, **Galling, U.** and **Michaelis, W.** (1997) Organic matter in Great Salt Lake ooids (Utah, USA) – first approach to a formation via organic matrices. *Facies*, **36**, 210–219.

Richter, D.K. (1983) Calcareous ooids: A synopsis. In: *Coated Grains* (Ed Peryt, T.M.), pp. 71–99. Springer, Berlin.

Rothpletz, A. (1892) On the formation of oölite. *Am. Geol.*, **10**, 279–282.

Scholze, F., **Wang, X.**, **Kirscher, U.**, **Kraft, J.**, **Schneider, J.W.**, **Götz, A.E.**, **Joachimski, M.M.** and **Bachtadse, V.** (2017) A multistratigraphic approach to pinpoint the Permian-Triassic boundary in continental deposits: The Zechstein–Lower Buntsandstein transition in Germany. *Global Planet. Change*, **152**, 129–151.

Scotese, C. (2021) An atlas of Phanerozoic paleogeographic maps: the seas come in and the seas go out. *Annu. Rev. Earth Planet. Sci.*, **49**, 679–728.

Shroder, J.F., **Cornwell, K.**, **Oviatt, C.G.** and **Lowndes, T.C.** (2016) Landslides, alluvial fans, and dam failure at Red Rock Pass: the outlet of Lake Bonneville. In: *Lake Bonneville: A Scientific Update* (Eds Oviatt, C.G. and Shroder, J.F.), pp. 75–85. Elsevier, Amsterdam.

Siahi, M., **Hofmann, A.**, **Master, S.**, **Mueller, C.W.** and **Gerdes, A.** (2017) Carbonate ooids of the Mesoarchaean Pongola Supergroup, South Africa. *Geobiology*, **15**, 750–766.

Simone, L. (1981) Ooids: a review. *Earth-Sci. Rev.*, **16**, 319–355.

Stampfli, G.M. (2000) Tethyan oceans. In: *Tectonics and Magmatism in Turkey and the Surrounding Area* (Eds Bozkurt, E., Winchester, J.A. and Piper, J.D.A.), *Geological Society, London, Special Publications*, **173**, 1–23.

Strasser, A. (1986) Ooids in Purbeck limestones (lowermost Cretaceous) of the Swiss and French Jura. *Sedimentology*, **33**, 711–727.

Suarez-Gonzalez, P. and **Reitner, J.** (2021) Ooids forming *in situ* within microbial mats (Kiritimati atoll, central Pacific). *PalZ*, **95**, 809–821.

Suess, E. and **Fütterer, D.** (1972) Aragonitic ooids: experimental precipitation from seawater in the presence of humic acid. *Sedimentology*, **19**, 129–139.

Summons, R.E., **Bird, L.R.**, **Gillespie, A.L.**, **Pruss, S.B.**, **Roberts, M.** and **Sessions, A.L.** (2013) Lipid biomarkers in ooids from different locations and ages: evidence for a common bacterial flora. *Geobiology*, **11**, 420–436.

Sumner, D.Y. and **Grotzinger, J.P.** (1993) Numerical modeling of ooid size and the problem of Neoproterozoic giant ooids. *J. Sediment. Petrol.*, **63**, 974–982.

Trichet, J. and **Défarge, C.** (1995) Non-biologically supported organomineralization. *Bulletin de l'Institut Océanographique (Monaco) Numéro Spécial*, **14**, 203–236.

Trower, E.J., **Lamb, M.P.** and **Fischer, W.W.** (2017) Experimental evidence that ooid size reflects a dynamic equilibrium between rapid precipitation and abrasion rates. *Earth Planet. Sci. Lett.*, **468**, 112–118.

Trower, E.J., **Cantine, M.D.**, **Gomes, M.L.**, **Grotzinger, J.P.**, **Knoll, A.H.**, **Lamb, M.P.**, **Lingappa, U.**, **O'Reilly, S.S.**, **Present, T.M.**, **Stein, N.**, **Strauss, J.V.** and **Fischer, W.W.** (2018) Active ooid growth driven by sediment transport in a high-energy shoal, Little Ambergris Cay, Turks and Caicos Islands. *J. Sediment. Res.*, **88**, 1132–1151.

Trower, E.J., **Bridgers, S.L.**, **Lamb, M.P.** and **Fischer, W.W.** (2020) Ooid cortical stratigraphy reveals common histories of individual co-occurring sedimentary grains. *J. Geophys. Res. Earth*, **125**, e2019JF005452.

Vennin, E., **Bouton, A.**, **Bourillot, R.**, **Pace, A.**, **Roche, A.**, **Brayard, A.**, **Thomazo, C.**, **Virgone, A.**, **Gaucher, E.C.**, **Desaubliaux, G.** and **Visscher, P.T.** (2019) The lacustrine microbial carbonate factory of the successive Lake Bonneville and Great Salt Lake, Utah, USA. *Sedimentology*, **66**, 165–204.

Volkmann, G.A. (1720) *Silesia Subterranea*, p. 347. Weidmann, Leipzig.

Weber, G.H., **Lukeneder, A.**, **Harzhauser, M.**, **Mitteroecker, P.**, **Wurm, L.**, **Hollaus, L.M.**, **Kainz, S.**, **Haack, F.**, **Antl-Weiser, W.** and **Kern, A.** (2022) The microstructure and the origin of the Venus from Willendorf. *Sci. Rep.*, **12**, 2926.

Weidlich, O. (2007) PTB mass extinction and earliest Triassic recovery overlooked? New evidence for a marine origin of Lower Triassic mixed carbonate–siliciclastic sediments (Rogenstein Member), Germany. *Palaeogeogr. Palaeoclimatol. Palaeoecol.*, **252**, 259–269.

Wingender, J., **Neu, T.R.** and **Flemming, H.-C.** (1999) What are bacterial extracellular polymeric substances? In: *Microbial Extracellular Polymeric Substances* (Eds Wingender, J., Neu, T.R. and Flemming, H.-C.), pp. 1–19. Springer, Berlin Heidelberg.

Woods, A.D. (2013) Microbial ooids and cortoids from the Lower Triassic (Spathian) Virgin Limestone, Nevada, USA: Evidence for an Early Triassic microbial bloom in shallow depositional environments. *Global Planet. Change*, **105**, 91–101.

Ziegler, P.A. (1990) *Geological Atlas of Western and Central Europe*, pp. 1–239. Geological Society Publishing House, Bath.

Manuscript received 10 July 2023; revision accepted 6 January 2024